

# Van der Pauw device used to investigate the thermoelectric power factor

Cite as: Rev. Sci. Instrum. **91**, 115102 (2020); <https://doi.org/10.1063/5.0019005>

Submitted: 20 June 2020 • Accepted: 14 October 2020 • Published Online: 03 November 2020

 Sebastian Haupt, Frank Edler, Markus Bartel, et al.



View Online



Export Citation



CrossMark

## ARTICLES YOU MAY BE INTERESTED IN

[Data analysis for Seebeck coefficient measurements](#)




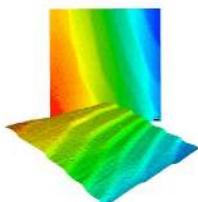

Review of Scientific Instruments **84**, 065102 (2013); <https://doi.org/10.1063/1.4807697>

[A setup to measure the Seebeck coefficient and electrical conductivity of anisotropic thin-films on a single sample](#)

Review of Scientific Instruments **91**, 105111 (2020); <https://doi.org/10.1063/5.0021715>

[Efficient thermoelectric van der Pauw measurements](#)

Applied Physics Letters **99**, 022102 (2011); <https://doi.org/10.1063/1.3609325>

|   |  |  |   |  |
|---|--|--|---|--|
|  | <p>Nanopositioning Systems</p>  | <p>Modular Motion Control</p>  | <p>AFM and NSOM Instruments</p>  | <p>Single Molecule Microscopes</p>  |
|---|--|--|---|--|



# Van der Pauw device used to investigate the thermoelectric power factor

Cite as: Rev. Sci. Instrum. 91, 115102 (2020); doi: 10.1063/5.0019005

Submitted: 20 June 2020 • Accepted: 14 October 2020 •

Published Online: 3 November 2020



Sebastian Haupt,<sup>1,a)</sup>  Frank Edler,<sup>1</sup> Markus Bartel,<sup>2</sup> and Hans-Fridtjof Pernau<sup>2</sup> 

## AFFILIATIONS

<sup>1</sup>Physikalisch-Technische Bundesanstalt, Abbestraße 2-12, 10587 Berlin, Germany

<sup>2</sup>Fraunhofer-Institut für Physikalische Messtechnik IPM, Heidenhofstraße 8, 79110 Freiburg im Breisgau, Germany

<sup>a)</sup>Author to whom correspondence should be addressed: [sebastian.haupt@ptb.de](mailto:sebastian.haupt@ptb.de)

## ABSTRACT

In this paper, we describe a measuring system based on the Van der Pauw principle with four calibrated type S thermocouples. By means of this system, we conducted traceable measurements of the absolute Seebeck coefficients and the electrical conductivity of thermoelectric bulk materials to establish a precise determination of the power factor. The results of a comparative investigation of metallic (ISOTAN<sup>®</sup> and Nickel) and semiconducting (SiGe) materials in the temperature range of 300 K–1100 K are presented. The good agreement of the Seebeck coefficients and electrical conductivities measured using the system and the data reported from the literature and values of these transport properties premeasured using another measuring system forms the basis for the usage of the system for the further certification of thermoelectric reference materials for the power factor up to 1100 K.

© 2020 Author(s). All article content, except where otherwise noted, is licensed under a Creative Commons Attribution (CC BY) license (<http://creativecommons.org/licenses/by/4.0/>). <https://doi.org/10.1063/5.0019005>

## I. INTRODUCTION

Using thermoelectric materials, it is possible to convert heat directly into electrical energy; their advantages are that they contain no moving parts and that the conversion is completely silent.<sup>1</sup> Thermoelectric generators are particularly common in space applications and have proven operating times over decades.<sup>2</sup> The efficiency of the thermoelectric energy conversion scales with the thermoelectric figure of merit  $ZT = S^2\sigma T/\kappa$  ( $ZT$ ) of the material used, where  $S$ ,  $\sigma$ ,  $\kappa$ , and  $T$  are the Seebeck coefficient, the electrical conductivity, the thermal conductivity, and the thermodynamic temperature, respectively. The cornerstone for a reliable assessment of thermoelectric materials is the precise determination of their thermoelectric transport properties. The evaluation of the transport properties based on suitable reference materials would enable reliable benchmarking of new thermoelectric materials. Therefore, thermoelectric reference materials and the associated measurement systems in the temperature range up to 1100 K are of great interest for the thermoelectric community. The recent increased focus on high-temperature thermoelectric applications has revealed a lack of reliable characterization techniques in the field of thermoelectricity, especially for the

Seebeck coefficient. Past comparative measurements have revealed deviations for individual thermoelectric properties of around 10%, which has led to a standard measurement uncertainty for the figure of merit  $ZT$  more than 12% ( $k = 1$ ).<sup>3–6</sup>

Our work is focused on the power factor defined as  $PF = S^2\sigma$ . This power factor is proportional to the output power and is thus important for the design of thermoelectric generators.<sup>7</sup>

The evaluation of the thermoelectric power factor (for instance, by using reference materials with known thermoelectric properties) is essential for validating testing methods and the main cornerstone for reliable benchmarking of thermoelectric materials. In general, reference materials are adequate for validating measuring systems and methods used to measure complex quantities such as the Seebeck coefficient. Due to the absence of standardized measurement protocols and fully traceable metrology, a wide variety of characterization techniques (most of which do not have estimated uncertainty budgets) have been used by many researchers. Therefore, it is necessary to develop traceable and robust methods to determine property data for thermoelectric materials.

The development of a measuring system is part of the TEST-HT (Thermoelectric Standardization for High Temperatures) project,

which has been funded by the German Federal Ministry of Education and Research (BMBF) and was started in 2018 as a collaboration between Physikalisch-Technische Bundesanstalt (PTB) and the German Aerospace Center (DLR). Creating a reliable thermoelectric measuring system for high temperatures is a challenging task for which different approaches have been tested in recent years: commercial systems [ZEM 3 (ULVAC), SB1000 (MMR Technologies), LSR-3 (LINSEIS), and SBA 458 Nemesis (Netzsch)<sup>8–11</sup>] and different research systems.<sup>12–18</sup> However, these systems are mainly focused on the Seebeck coefficient and therefore result in higher uncertainties for the electrical conductivity.<sup>4</sup> In principle, the Seebeck coefficient and the electrical conductivity are independent of the geometry. Therefore, the development of the reference material is only restricted on the use of suitable measurement techniques with known low uncertainties.

## II. Van der Pauw DEVICE (IPM-VdP)

For the certification of thermoelectric materials at PTB, the SRX measuring system from the IPM has been used to date.<sup>19–22</sup> Using this measuring system, the Seebeck coefficient of bulk materials and thin films can be measured precisely in the temperature range between 300 K and 850 K, but the accuracy of the measurement of the electrical conductivity is limited.

Good thermal and electrical contact between the thermocouples and the sample is important for the accuracy of the measurement of  $S$ . To achieve the best possible contact, non-sheathed thermocouples were used in the SRX measuring system at PTB. However, the direct contact with the sample proved to be unsatisfactory due to the risk of damaging the thermocouples and the sample.<sup>20</sup> Hence, for better manageability and to reduce downtime in the facility, our new Van der Pauw device uses mineral-insulated metal-sheathed (MIMS) thermocouples that are equipped with platinum/rhodium (Pt10%Rh) shields. However, the shields also impair contact with the sample and increase the parasitic heat flow. A new measuring system, IPM-VdP 1100 K, has been designed to realize the Van der Pauw principle to measure electrical conductivity with higher accuracy. The Van der Pauw principle provides an accurate measurement of the electrical conductivity of a sample of any arbitrary shape if the four probes are placed on the sample's perimeter and the sample is approximately two-dimensional.<sup>23</sup> Recently, it is also used to measure thermoelectric properties.<sup>24</sup>

To this end, this system's four shielded type S thermocouples are arranged in a square of 10 mm side length. The position of the thermocouples is fixed, and therefore, samples smaller than 10 mm cannot be measured with the Van der Pauw principle. However, the Seebeck coefficient of a bar shaped sample with a minimum length of 10 mm and a minimum width of 1 mm can be measured. The advantage of a fixed geometry for the thermocouples is a lower uncertainty due to accidental changes in the positions of the thermocouples.

The thermocouples are used to measure the temperature of the sample and all occurring voltages (i.e., the thermovoltages that result from the applied temperature gradient, as well as the electrical voltages from the conductivity measurement). The choice of the probes used plays an important role in the attainable uncertainty and defines the useful temperature range of the measurement. A photo of the measurement setup is shown in Fig. 1, and a schematic of the holder is displayed in Fig. 2. The type S thermocouples are calibrated

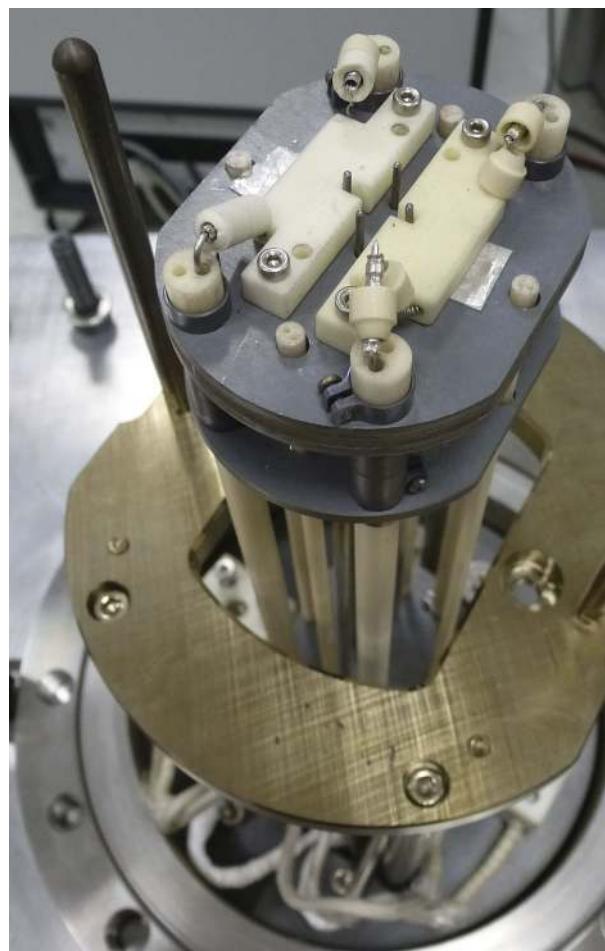


FIG. 1. Picture of the IPM-VdP 1100 K measurement setup with four calibrated type S thermocouples in a square configuration and two Shapal sample holders.

at PTB against fixed points to ensure the traceability of the temperature measurement to the International Temperature Scale of 1990 (ITS-90).

The calibration of the thermocouples reduces the uncertainty for the measurements of the temperature gradient and of the sample temperature. The sheathed thermocouples have an outer diameter of 1 mm and a length of about 600 mm. They are pressed against the sample from far below by means of springs. Due to the large distance from the heater, the temperature of the springs is only slightly above room temperature, and therefore, there is no loss of spring force.

Due to the relatively high pressure, a careful fitting of the sample into the holder is necessary to avoid the breakage of brittle samples. Two of the thermocouples are inside the sample holders, which are made of Shapal (sintered form of boron nitride and aluminum nitride) (see Fig. 1). The two holders are equipped with resistance heaters (coiled nickel–copper wires) that generate the required temperature gradient for the measurement of the Seebeck coefficient. The sample is fixed in position with two SiN beams and four molybdenum screws that are connected to the SiN support

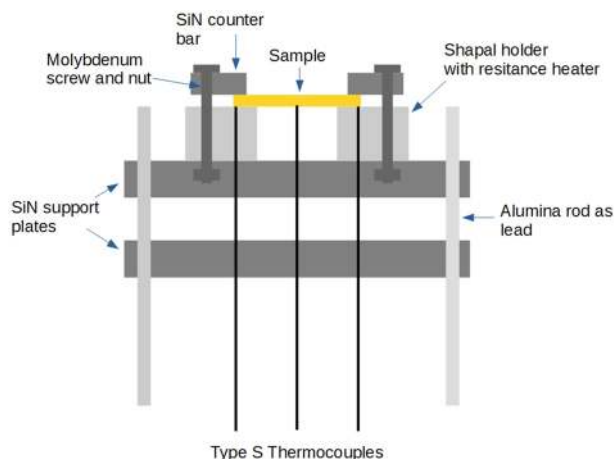


FIG. 2. Schematic of the sample holder of the IPM-VdP 1100 K measurement setup.

plates. Molybdenum screws and nuts were used due to the high-temperature stability of molybdenum, which were found to be superior to steel screws. The reference temperature of the thermocouples was measured with a calibrated Pt-100 resistance thermometer. The setup was placed in a vacuum chamber under the low pressure of an inert atmosphere ( $N_2$  with an admixture of  $H_2$ ) of  $\sim 60$  mbars. All occurring voltages were measured with a calibrated Keithley 2701 multimeter and a 7702 differential multiplexer card. The sample was heated with a ceramic heater that surrounded the sample and the holder completely. The Seebeck coefficient, as well as the electrical conductivity, was measured during the heating phases and during the cooling of the measuring facility.

### A. Measurement of the Seebeck coefficient

To measure the unknown Seebeck coefficient of a sample, a temperature difference  $\Delta T = T_1 - T_2$  was induced across the sample by means of small resistance heaters inside the Shapal holder. The two sides of the sample were heated in sequence. The type S thermocouples were electrically and thermally coupled to the sample and measured the occurring voltages and the temperature difference  $\Delta T$ . To ensure that the measurements were not affected by unavoidable offset voltages or by single erroneous values of the gradient applied to the sample, a dynamical measurement mode was used. The principle of the setup is described in detail by Burkov *et al.*<sup>17</sup> and by Boffoué *et al.*<sup>16</sup> Based on the known absolute Seebeck coefficient of the thermoelements (Pt and PtRh10%, respectively), the unknown Seebeck coefficient of the sample was calculated from the measured temperature difference and voltage,

$$S_X = \frac{1}{2} (a_{Pt/X} + a_{PtRh/X} + S_{Pt} + S_{PtRh}). \quad (1)$$

Here,  $S_X$  represents the unknown Seebeck coefficient of the sample X. The slopes  $a_{Pt/X}$  and  $a_{PtRh/X}$  are generated by means of the linear regression of data points arising from plotting the thermal voltage vs the temperature difference  $V_{Pt/X}/\Delta T$  and  $V_{PtRh/X}/\Delta T$  with respect to the materials Pt and PtRh10% over the sample X. Typically, about 140 data points are used to calculate each linear regression.  $S_{Pt}$  and  $S_{PtRh}$  represent the absolute Seebeck coefficients of Pt and PtRh10%,

respectively. The values of  $S_{Pt}$  were taken from the study of Roberts *et al.*<sup>25</sup> and were interpolated using a six-order polynomial. The absolute Seebeck coefficient for PtRh10% was calculated from the Roberts values and from coefficients of the type S reference function<sup>26</sup> with the help of a six-order polynomial. The maximum temperature gradient over the sample was defined in the software; for the measurements in this work, it was set to 5 K. In some measurements, this maximum gradient was not reached; in this case, heating of the sample was stopped after 150 s for each side.

The combined measurement uncertainty of the Seebeck coefficient  $u(S_X)$  at a certain temperature is the square root of the combined variance  $u^2(S_X)$ , given by

$$u^2(S_X) = \frac{1}{4} (u^2(a_{Pt/X}) + u^2(a_{PtRh/X}) + u^2(S_{Pt}) + u^2(S_{PtRh})). \quad (2)$$

The full uncertainty budget meets the mandatory regulation of the International Organization for Standardization on an unspecified material outlined in Ref. 27. In this work, we use combined measurement uncertainties ( $k = 1$ ) with a level of confidence of  $\sim 70\%$ . Usually, the level of confidence will be increased to 95% with an expansion of the used uncertainties to  $k = 2$ , which means a doubling of the stated uncertainties.

A detailed uncertainty analysis of Seebeck coefficient measurements by using Au/Pt thermocouples can be found.<sup>19</sup> The different contributions to the uncertainty of the slopes  $a$  are the uncertainties of the regression lines of the slopes, of the calibration of the thermocouples, of the thermal contact, of the electrical measurements, and of the temperature difference. The use of calibrated type S thermocouples instead of non-calibrated gold platinum direct thermocouples results only in a few modifications to the Au/Pt budget. We presume that the uncertainty of the absolute Seebeck coefficient for PtRh10% is equal to the uncertainty of  $S_{Au}$ . Since we have calibrated our thermocouples, we use the calibration uncertainties of 0.8 K instead of the assumed 2 K for the not calibrated Au/Pt thermocouples. Due to a different multimeter, the uncertainty of the voltage drops to  $1.2 \mu V$ . The dominating contribution to the uncertainty for materials with a low Seebeck coefficient such as metals is the uncertainty of the electrical measurement. For material with a higher Seebeck coefficient, the impairment of temperature measurement is caused by parasitic heat fluxes along the thermocouples and radiation effects. In total, we estimate a similar uncertainty for the new Van der Pauw device as for the IPM-SRX measuring system.

### B. Measurement of the electrical conductivity

A square configuration of the four probes was implemented to allow the Van der Pauw method to be used to measure the electrical conductivity.<sup>28–31</sup> The advantage of this method is that it provides an accurate measurement of the conductivity of a sample of any arbitrary shape if the four probes are placed on the sample's perimeter and the sample is approximately two-dimensional. The current was applied to two adjacent sides of the sample, and the voltage was measured at the opposite side of the current contacts. By a cyclic rotation of the current and voltage connections to the edges of the sample, four different measurements of the resistance ( $R_{12}, R_{34}, R_{23}, R_{41}$ ) can be made. Presuming a perfect sample and ideal contacts, the four resistance measurements give equal results. Van der Pauw proved that from the measured resistance values, the sheet conductivity can

be derived according to

$$1 = \exp(-\sigma_X R_A/d) + \exp(-\sigma_X R_B/d). \quad (3)$$

Here,  $R_A$  and  $R_B$  are the mean values  $R_A = (R_{12} + R_{34})/2$  and  $R_B = (R_{23} + R_{41})/2$  and  $d$  is the thickness of the sample. For the application of the VdP theorem, the homogeneity of the plate sample with respect to its conductivity is indispensable. Equation (3) can be rewritten with the help of the function  $f$  as

$$\frac{1}{\sigma_X} = \frac{\pi d}{\ln 2} \frac{R_A + R_B}{2} f(R_A/R_B) G. \quad (4)$$

The function  $f$  is a correction factor, which takes into account that the sample is not perfectly quadratic and only depends on the ratio of the resistance and is equal to unity within 0.001% if the resistances are equal within 1%. Furthermore, it is to be considered that the positions of the thermocouples are fixed and therefore not necessarily at the edge of the sample. Moreover, the diameter of the shielded thermocouples is about 1 mm relatively large for the samples. Hence, to obtain precise values of the electrical conductivity, each conductivity value must be corrected by an additional geometric factor  $G$ .<sup>26</sup> These correction factors were calculated at the Fraunhofer IPM by means of finite element simulations using COMSOL<sup>®</sup>-Multiphysics based on a method that uses the principle image charges<sup>28</sup> and is described in detail by Ilse *et al.*<sup>29</sup>

It should be noted that the thermal expansion of the sample is not considered in the uncertainty analysis. For instance, changes in the distance between the thermocouples held by the ceramic plates could have a stronger impact on the measurement than a change of the sample itself by thermal expansion. In addition, the sample (and the thermocouples) is held in position by molybdenum screws with a different thermal expansion. It is possible that when expansion effects occur in different directions, a partial compensation of these effects takes place. This is the main reason why we observed no drift effects but more scattering of the results due to thermal expansion.

In the Van der Pauw method, the probes must form an ohmic contact to the sample. The IPM-VdP 1100 K system offers different methods of measuring the electrical conductivity to verify this ohmic contact. The quality of the contacts can be assessed by comparing the measurements. In this work, we present electrical conductivity values obtained by means of a LakeShore 372 AC resistance bridge with a built-in lock-in amplifier. Additionally, a TTI TG5011A function generator enabled faster measurements of the conductivity during the voltage sweep process. This method has proven to be very sensitive to contact resistivity and was used to control the ohmic contact but not to measure the conductivity due to a high level of fluctuation. The third method is a simple current flow through the sample with the fixed currents and the measured voltages. This so-called delta mode can also be used to measure bar shape samples whose width is lower than 10 mm; however, this requires two additional connector plates from the sample to the outermost thermocouples to make the electrical contact.

The combined measurement uncertainty of the conductivity  $u(\sigma_X)$  at a certain temperature is the square root of the combined variance  $u^2(\sigma_X)$ , given by

$$u^2(\sigma_X) = \sigma_X^2 \left( \frac{u^2(d)}{d^2} + \frac{u^2(R_A)}{R_A^2} + \frac{u^2(R_B)}{R_B^2} + \frac{u^2(f)}{f^2} + \frac{u^2(G)}{G^2} \right). \quad (5)$$

The dominating contribution to the uncertainty for the electrical conductivity in our work is the uncertainty of the thickness of the sample. For the metallic samples, we have assumed an uncertainty contribution of 12  $\mu\text{m}$ . We use metallic samples with a thickness of less than 0.3 mm in our work to validate our measuring system. Therefore, we have a relative high uncertainty of up to 4% for these samples. For the SiGe sample, we use an uncertainty contribution of 6  $\mu\text{m}$  for the thickness. The uncertainty of the actual measurement of the resistances  $R_A$  and  $R_B$  is defined through the used resistance bridge and the temperature stability of the sample (about 0.25 K during a measurement). The temperature contribution is the lowest uncertainty contribution of about 0.1%. For the geometric factor, we consider an uncertainty contribution of 0.4% resulting from the uncertainty of sample geometry and the mounting of the samples.

The measurement uncertainty of the power factor of the measured sample  $X$  is the combination of the variances of the Seebeck coefficient and the electrical conductivity,

$$u^2(PF_X) = S_X^4 u^2(\sigma_X) + 4S_X^2 \sigma_X^2 u^2(S_X). \quad (6)$$

### III. SAMPLES

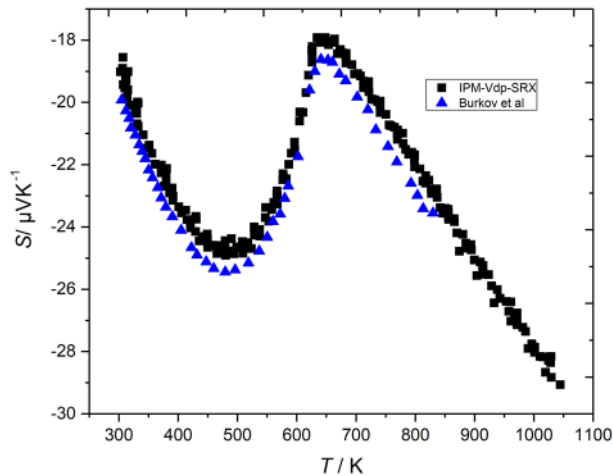
For a comparative investigation and validation of IPM-VdP 1100 K, three different materials were investigated regarding their power factors. The values of  $S$  and  $\sigma$  of an ISOTAN sample (a copper-nickel alloy made by Isabellenhütte Heusler,<sup>32</sup> 11.5 \* 11.5 \* 0.3 mm<sup>3</sup>, correction factor  $G = 0.9418$  for the measurement of  $\sigma$  from the COMSOL simulations) were compared with the values measured using our standard SRX equipment with non-sheathed noble-metal thermocouples.<sup>18</sup> A boron-doped SiGe sample (12 \* 12 \* 1.5 mm<sup>3</sup>, correction factor 0.9261) was provided by the Fraunhofer IPM and measured at temperatures up to 980 K. The germanium platinum eutectic point (around 1040 K) limited the maximum measurement temperature. The samples were cut from a disk with a diameter of 30 mm produced at the Leibniz Institute for crystal growth in Berlin. Furthermore, a pure nickel sample (99.95% nickel: 12 \* 12 \* 0.245 mm<sup>3</sup>; correction factor 0.9251) was measured at temperatures up to 1050 K.

### IV. SEEBECK COEFFICIENTS

The Seebeck coefficient (black squares) of a pure nickel sample measured four times in the temperature range from 300 K to 1044 K is displayed in Fig. 3.

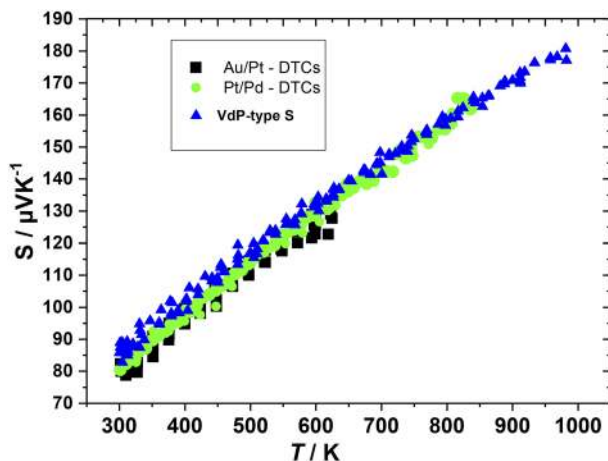
The measured Seebeck coefficients of the nickel sample agree well with the values given by Burkov *et al.*<sup>17</sup> (blue triangles) but are slightly lower by about 0.5  $\mu\text{V K}^{-1}$ , which is lower than the  $k = 1$  uncertainty of the measurement setup. One reason for this may be a difference in the quality of the nickel sample. The square root of the statistic variance of the measurements is about 0.24  $\mu\text{V K}^{-1}$ . Here and below, we give the root of the statistic variance to enable easy comparability. At the Curie temperature of 633 K, a clear local maximum of the Seebeck coefficient of about  $-18 \mu\text{V K}^{-1}$  appears. The measurement uncertainty ( $k = 1$ ) for the Seebeck coefficient is about 1.8  $\mu\text{V K}^{-1}$  (9.5%) at 303 K and 1.9  $\mu\text{V K}^{-1}$  (6.8%) at 1044 K.

Figure 4 shows the temperature dependence of the Seebeck coefficient of the SiGe sample in the temperature range from 300 K to 980 K. The sample was measured in six independent runs. The square root of the statistic variance of the SiGe measurements is



**FIG. 3.** Temperature dependence of the Seebeck coefficient of a pure nickel sample (black squares) measured with IPM-VdP. Values from the study of Burkov *et al.* (blue triangles)<sup>17</sup> were included for comparison.

about  $0.9 \mu\text{V K}^{-1}$ . For comparison purposes, the Seebeck coefficients measured using the IPM-SRX facility with non-sheathed Au/Pt thermocouples (black squares) and with non-sheathed Pt/Pd thermocouples (green circles) from Ref. 22 were included. Both thermocouple types for the IPM-SRX facility were in direct contact with the sample. At temperatures above 600 K, the Seebeck coefficients measured with the VdP facility and the SRX facility by using the Pt/Pd thermocouples agreed very well. At lower temperatures, the Seebeck coefficients measured using the VdP facility were higher [about  $5 \mu\text{V K}^{-1}$  at 303 K (6%)]. This difference corresponds to about the expanded uncertainty ( $k = 2$ ) of  $4.6 \mu\text{V K}^{-1}$  and is lower than the expanded uncertainty by using Au/Pt thermocouples with the SRX device ( $7.2 \mu\text{V K}^{-1}$ ). Moreover, this difference is probably caused by



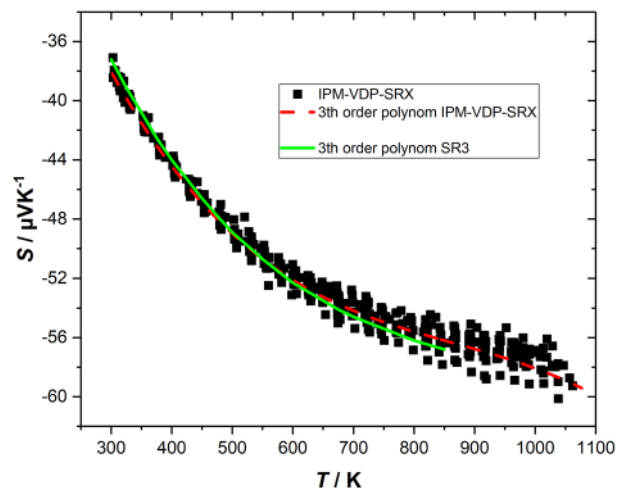
**FIG. 4.** Temperature-dependent Seebeck coefficient of the B-doped SiGe sample measured with IPM-VdP 1100 K (blue triangles). For comparison purposes, the Seebeck coefficients measured with the SRX and bare Au/Pt thermocouples (black squares) and bare Pt/Pd thermocouples (green circles) from Ref. 22 are included.

a different level of boron doping, since the square sample measured with the VdP facility was cut from a different disk and therefore from a different location within the SiGe crystal than the bar sample measured with the IPM-SRX facility. However, the differences in the doping level are neglectable due to temperature-induced charge carriers at higher temperatures. Hence, above 600 K, the Seebeck coefficients are almost identical.

The uncertainty ( $k = 1$ ) for the Seebeck coefficient of SiGe at 303 K is about  $2.3 \mu\text{V K}^{-1}$  (2.8%) and increases to circa  $2.6 \mu\text{V K}^{-1}$  (1.6%) at 968 K.

Although the contact between the sample and the sheathed thermocouples (VdP facility) is not as good as for the non-sheathed thermocouples (SRX), the measurement results were unaffected by these effects above 600 K, which indicates that the measurements are not strongly influenced by the different contact to the sample or the possible higher thermal flux through the sheathed thermocouples.

Figure 5 shows the temperature dependence of the Seebeck coefficient of ISOTAN in the temperature range from 300 K to 1060 K. In contrast to the other measurements in this work, where only one sample of a material was measured, the graph for the ISOTAN sample contains data of 11 independent measurements of three ISOTAN samples taken from the same batch (400 points). It is to be considered that the contacts between the samples and the thermocouples vary slightly, for each sample and for each run due to thermal expansion. Therefore, the measurements show some scattering especially at high temperature due to high thermal stress. However, the statistic variance of the measurements is still low of about  $0.5 \mu\text{V K}^{-1}$  (root of the variance). The graph contains two lines: the red dashed line corresponds to a three-order polynomial fit of the values measured with IPM-VdP up to 1060 K. The solid green line corresponds to a three-order fit based on the values measured using the IPM-SRX facility with bare Au/Pt thermocouples.<sup>21</sup> For ISOTAN, we calculate an uncertainty ( $k = 1$ ) for the Seebeck coefficient of about  $1.8 \mu\text{V K}^{-1}$  (4.7%) at 304 K and  $1.9 \mu\text{V K}^{-1}$  (3.3%) at 1028 K.



**FIG. 5.** Seebeck coefficient of an ISOTAN sample in the temperature range from 300 K to 1060 K with two three-order polynomial fits, red dashed line for the current facility and solid green line for the older IPM-SR5 facility with Au/Pt thermocouples.

Similarly, the green three-order polynomial fit for the IPM-SRX values is based on six different samples.<sup>19</sup> Despite the different kinds of thermocouples (and, hence, the different kinds of contacts to the sample), the average difference of the two polynomial curves is about  $0.2 \mu\text{V K}^{-1}$  (0.5%) with a maximum difference of  $0.8 \mu\text{V K}^{-1}$  (1.8%), which is distinctly lower than the uncertainty of the measurements.<sup>19</sup>

## V. ELECTRICAL CONDUCTIVITY

The measured values of the electrical conductivity were obtained with a LakeShore 372 AC resistance bridge that had a built-in lock-in amplifier based on the Van der Pauw principle. Figure 6 shows the temperature dependence of the electrical conductivity of the pure nickel sample at temperatures up to 1040 K (black diamonds).

The square root of the statistic variance of the nickel conductivity measurements is about  $260 \text{ Scm}^{-1}$ . The results of Ponnambalam *et al.*<sup>14</sup> (green circles) and of Burkov *et al.*<sup>17</sup> (blue triangles) were also included in the graph. At the Curie temperature of about 633 K, the slope of the conductivity curve abruptly decreases, indicating the phase transition of nickel. Overall, the results agreed well, even though our measured conductivity was slightly lower.

The uncertainty ( $k = 1$ ) for the electrical conductivity is about  $6375 \text{ Scm}^{-1}$  (4.9%) at 303 K and decreases to about  $1153 \text{ Scm}^{-1}$  (4.9%) at 1044 K. The dominated factor by far in the case of the nickel sample is the uncertainty of the thickness of the sample.

Figure 7 shows the temperature dependence of the electrical conductivity of an ISOTAN sample in the temperature range from 300 K to 1020 K. The conductivity was stable at a value of about  $20000 \text{ S/cm}$  up to about 633 K (nickel is the main component). At higher temperatures, the conductivity started to decrease. For purposes of visual orientation, a red dashed line is included in the figure. The square root of the statistic variance of the ISOTAN measurements is about  $80 \text{ Scm}^{-1}$ . In relative terms, the conductivity has a higher variation than that for nickel. The reasons for this are the

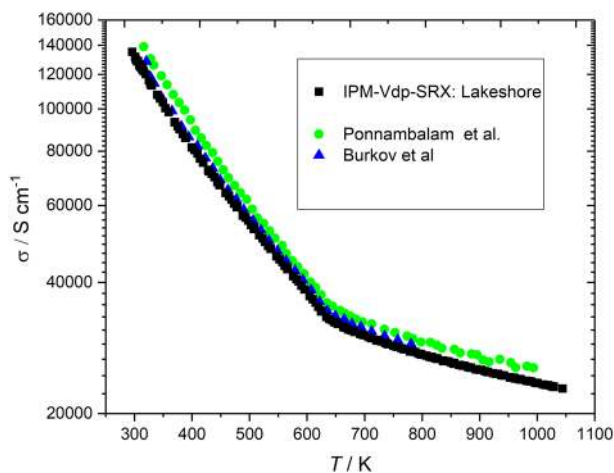


FIG. 6. Electrical conductivity of a nickel sample in the temperature range from 300 K to 1040 K. For comparison purposes, values from the study of Burkov *et al.*<sup>17</sup> (blue triangles) and Ponnambalam *et al.*<sup>14</sup> were included.

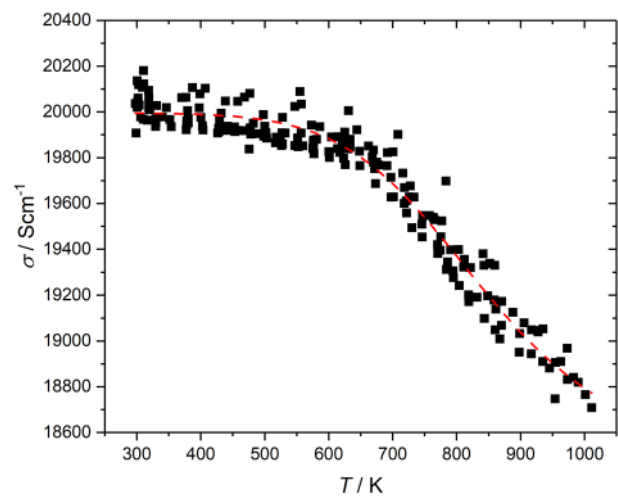


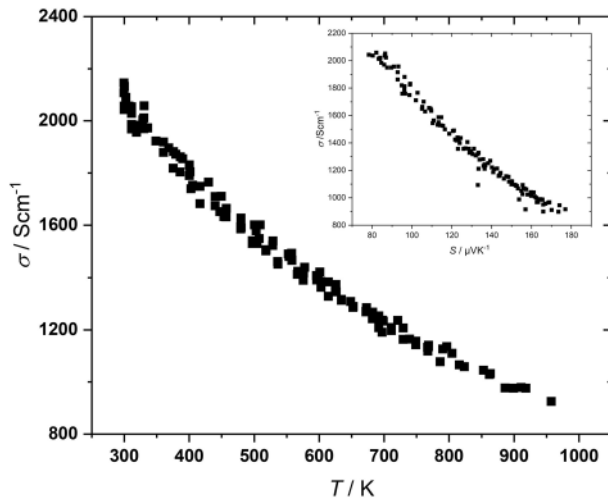
FIG. 7. Electrical conductivity of an ISOTAN sample in the temperature range from 300 K to 1020 K. The graph includes a red dashed line for purposes of visual orientation.

higher sensitivity against oxidation due to the copper fraction and a slight deformation of the thin sample due to the contact pressure of the thermocouples at higher temperatures. Although neither effect has a noticeable influence on the Seebeck coefficient, both effects challenge the suitability of ISOTAN as a high-temperature reference material (above 800 K) for the power factor. Like the nickel sample, the uncertainty ( $k = 1$ ) of  $\sigma$  is dominated by the uncertainty of the thickness of the sample at 304 K, which is about  $943 \text{ Scm}^{-1}$  (4.7%) and decreases to about  $872 \text{ Scm}^{-1}$  (4.6%) at 1028 K.

The electrical conductivity of the SiGe sample is displayed in Fig. 8 at temperatures up to 950 K. The conductivity undergoes a steady decrease with rising temperatures. The square root of the statistic variance of the SiGe measurements is about  $28 \text{ Scm}^{-1}$ . The electrical conductivity has an almost linear correlation with the Seebeck coefficient (see the inset in Fig. 8). For  $\sigma$ , we estimated an uncertainty of about  $55 \text{ Scm}^{-1}$  (2.4%) at 303 K, which decreases to circa  $29 \text{ Scm}^{-1}$  (3.0%) at 968 K.

The Seebeck coefficient and the electrical conductivity can be combined to obtain the power factor  $PF = S^2\sigma$ . The power factor of all measured materials is shown in Fig. 9. The power factor for ISOTAN (black squares) increases sharply at temperatures up to 700 K, while at higher temperatures, the factor is relatively constant.

Due to the higher number of measurements and the three different samples used for the ISOTAN measurements, the variation is higher than that for the single sample measurements of nickel and SiGe. A polynomial fit (red dashed line) was included for ISOTAN. The power factor of nickel (blue triangles) has a clear minimum at the Curie temperature; at room temperature, nickel has the highest value of all three materials due to its high electrical conductivity. The SiGe power factor (green dots) was the lowest of the three materials investigated (up to 560 K) in contrast to the Seebeck coefficient, which has the highest value of the materials. However, since SiGe has the lowest thermal conductivity of the three materials (about 6

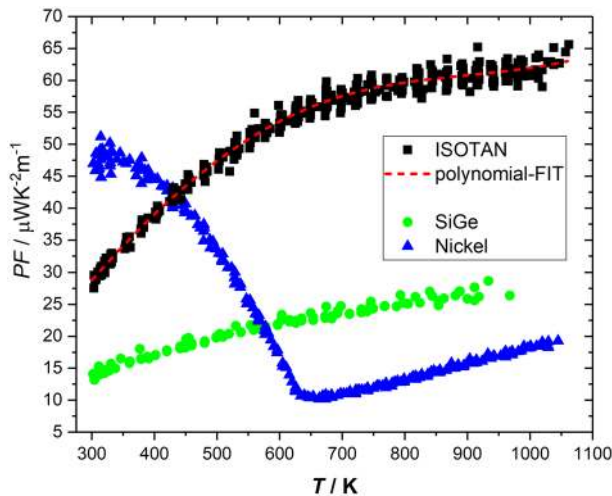


**FIG. 8.** Electrical conductivity of the B-doped SiGe sample measured in the temperature range from 300 K to 980 K. The inset shows the almost linear correlation of  $\sigma$  with the Seebeck coefficient.

W/mK at 300 K measured at the IPM on the intact disk), it still has the highest  $ZT$  value.

The uncertainty of the power factors for the samples is stated in Table I. The uncertainty for the metallic samples is quite large, which reflects an inauspicious combination of thin samples with low Seebeck coefficients. In contrast, SiGe proved to be a good choice for measurement of the power factor with a maximum uncertainty of 6.1% ( $k = 1$ ).

The relative uncertainties of the Seebeck coefficients and the electrical conductivities of the materials investigated are summarized in Table II.



**FIG. 9.** Power factors of ISOTAN (black squares), SiGe (green dots), and nickel (blue triangles) in the temperature range from 303 K to 1080 K. For ISOTAN, a polynomial fit (red dashed line) is included.

**TABLE I.** Uncertainty of the power factors ( $k = 1$ ) for the investigated samples in absolute and relative units.

| Material         | $\mu\text{W K}^{-2} \text{m}^{-1}$ | %    |
|------------------|------------------------------------|------|
| Nickel at 304 K  | 9.18                               | 19.6 |
| Nickel at 1044 K | 2.6                                | 14.3 |
| ISOTAN at 304 K  | 3.09                               | 10.5 |
| ISOTAN at 1028 K | 5.08                               | 8.0  |
| SiGe at 303 K    | 0.82                               | 6.1  |
| SiGe at 968 K    | 1.18                               | 4.4  |

**TABLE II.** Relative uncertainties of the Seebeck coefficient and of the electrical conductivity for  $k = 1$ .

| Material         | $u(S)$ (%) | $u(\sigma)$ (%) |
|------------------|------------|-----------------|
| Nickel at 304 K  | 9.5        | 4.9             |
| Nickel at 1044 K | 6.8        | 4.9             |
| ISOTAN at 304 K  | 4.7        | 4.7             |
| ISOTAN at 1028 K | 3.3        | 4.6             |
| SiGe at 303 K    | 2.8        | 2.4             |
| SiGe at 968 K    | 1.6        | 3.0             |

## VI. CONCLUSION

In this work, we have described a new four-point measurement system to measure the thermoelectric power factor based on the Van der Pauw method and have shown results for three different materials. The results demonstrate that our measurements agree well with literature values as well as with measurements performed using our standard SRX facility with bare thermocouples. The combination of the measurements of the Seebeck coefficients and the measurements of the electrical conductivity to the power factor provides a wider perspective on the materials investigated. Although the obtained uncertainties for the thin metallic samples were relatively high, the investigation of SiGe proved that with a thicker semi-conducting sample, a satisfying uncertainty level can be achieved. Hence, the IPM-VdP 1100 K measuring system creates an excellent basis for obtaining traceable and precise measurements that can be used in the certification of thermoelectric reference materials for the power factor, which will be the topic of future research.

## ACKNOWLEDGMENTS

This work was carried out within the scope of the TEST-HT (Thermoelectric Standardization for High Temperatures) project, a collaboration between Physikalisch-Technische Bundesanstalt (PTB) and the German Aerospace Center (DLR). This work was financed by the German Federal Ministry of Education and Research (BMBF) under Grant Nos. 03VP04402 (PTB) and 03VP04401 (DLR).

## DATA AVAILABILITY

The data that support the findings of this study are available from the corresponding author upon reasonable request.



## REFERENCES

- <sup>1</sup>D. M. Rowe, *CRC Handbook of Thermoelectrics*, edited by D. M. Rowe (CRC Press Inc., Boca Raton, 1995), p. 2.
- <sup>2</sup>G. Karacaloğlu, *Energy Resources for Space Missions* (Space Safety Magazine, 2014), <http://www.spacesafetymagazine.com/aerospace-engineering/nuclear-propulsion/energy-resources-space-missions>; accessed 8 January 2020.
- <sup>3</sup>N. D. Lowhorn, W. Wong-Ng, Z. Q. Lu *et al.*, “Development of a Seebeck coefficient standard reference material,” *Appl. Phys. A* **96**, 511–514 (2009).
- <sup>4</sup>E. Alleno *et al.*, “Invited article: A round robin test of the uncertainty on the measurement of the thermoelectric dimensionless figure of merit of  $\text{Co}_{0.97}\text{Ni}_{0.03}\text{Sb}_3$ ,” *Rev. Sci. Instrum.* **86**, 011301 (2015).
- <sup>5</sup>H. Wang, W. D. Porter, H. Böttner *et al.*, “Transport properties of bulk thermoelectrics—An international round-robin study, part I: Seebeck coefficient and electrical resistivity,” *J. Electron. Mater.* **42**, 654–664 (2013).
- <sup>6</sup>H. Wang, S. Bai, L. Chen *et al.*, “International round-robin study of the thermoelectric transport properties of an *n*-type half-Heusler compound from 300 K to 773 K,” *J. Electron. Mater.* **44**, 4482–4491 (2015).
- <sup>7</sup>W. Liu, H. S. Kim, Q. Jie, and Z. Ren, “Importance of high power factor in thermoelectric materials for power generation application: A perspective,” *Scr. Mater.* **111**, 3 (2016).
- <sup>8</sup>See <https://www.ulvac.com/components/Thermal-Instruments/Thermoelectric-Testers/ZEM-3-Series> for information about the ZEM-3 measurement unit.
- <sup>9</sup>See [http://www.mmr-tech.com/comp\\_seebeck\\_control.php](http://www.mmr-tech.com/comp_seebeck_control.php) for information about the SB1000 Digital Seebeck Effect Controller.
- <sup>10</sup>See <https://www.linseis.com/en/products/thermoelectrics/lsr-3/> for information about the LSR-3 Platform.
- <sup>11</sup>See <https://www.netzsch-thermal-analysis.com/en/products-solutions/seebeck-coefficient-electrical-conductivity/sba-458-nemesis/> for information about the SBA 458 Nemesis measurement setup.
- <sup>12</sup>L. Abadlia, F. Gasser, K. Khalouk, M. Mayoufi, and J. G. Gasser, “New experimental methodology, setup and LabView program for accurate absolute thermoelectric power and electrical resistivity measurements between 25 and 1600 K: Application to pure copper, platinum, tungsten, and nickel at very high temperatures,” *Rev. Sci. Instrum.* **85**, 095121 (2014).
- <sup>13</sup>Q. Fu, Y. Xiong, W. Zhang, and D. Xu, “A setup for measuring the Seebeck coefficient and the electrical resistivity of bulk thermoelectric materials,” *Rev. Sci. Instrum.* **88**, 095111 (2017).
- <sup>14</sup>V. Ponnambalam, S. Lindsey, N. S. Hickman, and T. M. Tritta, “Sample probe to measure resistivity and thermopower in the temperature range of 300–1000 K,” *Rev. Sci. Instrum.* **77**, 073904 (2006).
- <sup>15</sup>J. Martin, “Apparatus for the high temperature measurement of the Seebeck coefficient in thermoelectric materials,” *Rev. Sci. Instrum.* **83**(6), 065101 (2012).
- <sup>16</sup>O. Boffoué, A. Jacquot, A. Dauscher, B. Lenoir, and M. Stölzer, “Experimental setup for the measurement of the electrical resistivity and thermopower of thin films and bulk materials,” *Rev. Sci. Instrum.* **76**, 053907 (2005).
- <sup>17</sup>A. T. Burkov, A. Heinrich, P. P. Konstantinov, T. Nakama, and K. Yagasaki, “Experimental set-up for thermopower and resistivity measurements at 100–1300 K,” *Meas. Sci. Technol.* **12**, 264 (2001).
- <sup>18</sup>S. Iwanaga, E. S. Toberer, A. LaLonde, and G. J. Snyder, “A high temperature apparatus for measurement of the Seebeck coefficient,” *Rev. Sci. Instrum.* **82**(6), 063905 (2011).
- <sup>19</sup>F. Edler, E. Lenz, and S. Haupt, “Reference material for Seebeck coefficients,” *Int. J. Thermophys.* **36**, 482–492 (2015).
- <sup>20</sup>P. Ziolkowski, C. Stiewe, J. de Boor, I. Druschke, K. Zabrocki, F. Edler, S. Haupt, J. König, and E. Mueller, “Iron disilicide as high-temperature reference material for traceable measurements of Seebeck coefficient between 300 K and 800 K,” *J. Electron. Mater.* **46**, 51–63 (2017).
- <sup>21</sup>E. Lenz, F. Edler, and P. Ziolkowski, “Traceable thermoelectric measurements of Seebeck coefficients in the temperature range from 300 K to 900 K,” *Int. J. Thermophys.* **34**, 1975 (2013).
- <sup>22</sup>S. Haupt and F. Edler, “Traceable measurements of Seebeck coefficients of thermoelectric materials by using noble metal thermocouples,” *Int. J. Thermophys.* **39**, 72 (2018).
- <sup>23</sup>L. J. van der Pauw, “A method of measuring specific resistivity and Hall effect of discs of arbitrary shape,” *Philips Res. Rep.* **13**, 174–182 (1958).
- <sup>24</sup>J. de Boor and V. Schmidt, “Efficient thermoelectric van der Pauw measurements,” *Appl. Phys. Lett.* **99**, 022102 (2011).
- <sup>25</sup>R. B. Roberts, “The absolute scale of thermoelectricity II,” *Philos. Mag. B* **43**(6), 1125–1135 (1981).
- <sup>26</sup>IEC 60584-1, Thermocouples—Part 1: EMF Specifications and Tolerances, ed. 3.0, Technical Committee 65B (2013).
- <sup>27</sup>*Guide to the Expression of Uncertainty in Measurement*, 2nd ed. (International Organization for Standardization, Geneva, 1995), [http://www.iso.org/iso/catalogue\\_detail.htm?csnumber=50461](http://www.iso.org/iso/catalogue_detail.htm?csnumber=50461).
- <sup>28</sup>F. M. Smits, “Measurement of sheet resistivities with the four-point probe,” *Bell Syst. Tech. J.* **37**(3), 711–718 (1958).
- <sup>29</sup>K. Ilse *et al.*, “Geometrical correction factors for finite-size probe tips in microscopic four-point-probe resistivity measurements,” *J. Appl. Phys.* **116**, 224509 (2014).
- <sup>30</sup>L. B. Valdes, “Resistivity measurements on germanium for transistors,” *Proc. IRE* **42**(2), 420–427 (1954).
- <sup>31</sup>G. Rietveld *et al.*, “DC conductivity measurements in the Van der Pauw geometry,” *IEEE Trans. Instrum. Meas.* **52**(2), 449–453 (2003).
- <sup>32</sup>See [https://www.isabellenhuetten.de/fileadmin/Daten/Praezisionslegierungen/Datenblaetter\\_Thermo/Englisch/ISOTAN.pdf](https://www.isabellenhuetten.de/fileadmin/Daten/Praezisionslegierungen/Datenblaetter_Thermo/Englisch/ISOTAN.pdf) for information about the ISOTAN and its properties.